

Energy and Throughput Trade-offs in Cellular Networks using Base Station Switching

Abhinav Kumar, *Member, IEEE*, and Catherine Rosenberg, *Fellow, IEEE*

Abstract—Base station operation consumes a lot of energy, a considerable amount of which can be saved by switching off base stations during low user demand (for example, at night). Base station switching (BSS) can result in loss in coverage if not performed properly. We show that coverage is closely related to scheduling via power management and that the bottleneck is typically the uplink. To save energy, we propose a set of BSS patterns, at a global system-level, that have the potential to provide full coverage if the appropriate schedulers are used. We further show that the existing benchmark uplink scheduling schemes do not provide full coverage when BSS is used in urban as well as rural macro-cell environments (the downlink benchmark scheduling scheme provides full coverage only for some of the BSS patterns). Hence, we propose novel scheduling schemes for both uplink and downlink that realistically model interference, ensure full coverage, and provide good energy-performance trade-offs for the proposed BSS patterns. We also present a low complexity high performance heuristic for the proposed uplink scheduler. Finally, we show the presented models and results can be used to quantify, offline, the energy-performance trade-offs under different operating scenarios.

Index Terms—Base station switching, cellular network, coverage, downlink, energy, LTE, throughput, uplink.

1 INTRODUCTION

The information and communication technology (ICT) sector is estimated to be responsible for around 2% of the global CO₂ emissions [1]. Within ICT, cellular networks are one of the biggest contributors [1]. Base stations (BSs) operations consume up to 80% of the energy required for the operation of a cellular network [2]. Hence, schemes that can possibly switch off some BSs, when demand is lower, are important from the perspective of saving energy, money, and reducing the carbon footprint. LTE cellular systems [3] are typically designed for providing full coverage and good performance for a given (nominal) user density. However, as shown in [4], [5], significant time periods can occur when the user density drops far below this nominal density (for example, during the nights or public holidays). As BSs consume the majority of the energy in a cellular network, significant gain in operational expenditure (OPEX) is possible by suitably turning off some BSs and expanding the coverage of the remaining BSs when user density is low [4], [5], [6].

Typically, the objective of a base station switching (BSS) framework is to achieve the best possible energy versus throughput trade-off while maintaining full coverage when user equipment (UE) density decreases. This can be achieved by minimizing the en-

ergy consumption while maintaining the throughput performance as in the nominal system. Alternatively, we can maximize the throughput performance for a given energy consumption. The past works that have tried to address this problem have the following limitations.

- They only focus on the downlink. The uplink being more power limited is the bottleneck.
- The interference is not realistically modeled. In particular, it is highly dependent on which BSs are active (both on the uplink and the downlink).
- They work with a simplistic and rigid scheduler that limits the possible energy versus performance trade-offs.

When a BS is switched off, it affects all its neighboring BSs, which have to take over the region no more covered by that BS, making coverage more difficult. We consider that the operator switches off BSs using predefined global BSS patterns (motivated from the frequency re-use patterns typically used in cellular networks) that have been designed off-line to offer full coverage with suitable scheduling schemes on the uplink and the downlink. Scheduling is critical to the efficient operation of a cellular network with BSS. Providing non-zero data rate to the UEs on the downlink/uplink depends on the downlink/uplink scheduler which is in charge of allocating resources (e.g., time, channels¹, power per channel) to the UEs. By switching off BSs, the system becomes more power-limited and hence it is important that, whenever required, the schedulers should be flexible enough

1. We use the terms channels and sub-channels interchangeably throughout the paper.

• A. Kumar is with the Department of Electrical Engineering, Indian Institute of Technology Hyderabad, Telangana, 502205 India.
C. Rosenberg is with the Department of Electrical and Computer Engineering, University of Waterloo, Waterloo, ON N2L 3G1 Canada.
E-mail: abhinavkumar@iith.ac.in, cath@uwaterloo.ca.

to allow power to be focused on the right number of channels. However, focusing power impacts the interference which, in turn, limits coverage. Many schedulers proposed in the literature allocate power in a rigid way and hence do not fare well when BSs are switched off. Hence, studying BSS will amount to proposing uplink and downlink schedulers. In summary, the issues of coverage, scheduling, power per channel, and interference are highly inter-dependent and they need to be studied jointly both on the uplink and the downlink to enable a large range of energy/performance trade-offs in BSS. This is the motivation of this work. More precisely, the contributions of this paper are as follows.

- We propose a framework to study the energy versus performance trade-offs that takes into account uplink and downlink, and models interference properly. The framework is based on a detailed system model and predefined global BSS patterns. We show that the BSS patterns' feasibility in terms of coverage is determined by the uplink.
- We propose two novel flexible schedulers (one for the downlink and one for the uplink) to allow better performance-energy trade-offs than the state of the art schedulers. However, this flexibility has a computational cost. We will show that this computational cost is negligible on the downlink, but not on the uplink. Hence, a low complexity high performance heuristic is proposed for the uplink scheduling scheme.
- We present performance-energy trade-off results, for a given user density, for uplink and downlink in urban as well as rural macro-cell environments and quantify the gain obtained from the proposed schemes with respect to the state of the art.

The rest of the paper is organized as follows. In Section II, the related work is presented. The system model, BSS patterns, and the problem formulation are described in Section III. In Section IV, we discuss several scheduling schemes and propose the new scheduling schemes for BSS. The numerical results are presented in Section V. Section VI provides some concluding remarks.

2 RELATED WORK

The issues pertaining to coverage, throughput, and energy trade-offs in BSS are discussed in [7]. A first-order approximation of the percentage of power that can be saved by switching off BSs in an urban macro-cell environment during low traffic periods while maintaining coverage is presented in [4]. A practical BSS algorithm that takes into consideration the incremental impact of switching off BSs one by one on the downlink performance in an urban macro-cell is proposed in [5], but the uplink performance and uplink coverage issues are not considered. In heterogeneous networks composed of cellular and wireless

TABLE 1
Mathematical Notations

Symbol	Definition
α_n^D	Fraction of the time allocated to a UE n on the downlink
A_{e_1/e_2}	BS switching pattern with e_1 out of e_2 BSs on
β	TDD time fraction for downlink
\mathcal{B}	Set of Sectors
δ_{e_1/e_2}	Coverage area of a sector for pattern A_{e_1/e_2}
Δ	BSs' coverage area
ES_{e_1/e_2}	% energy saving for pattern A_{e_1/e_2}
f	Mapping between SINR and MCS efficiency
G_{xr}^c	Channel gain for a transmitter x with respect to receiver r
γ_{rx}^c	SINR per channel for transmitter x with respect to receiver r
Γ	Throughput performance metric
I_{xr}^c	Interference on receiver r on data from transmitter x
\mathcal{L}	Set of locations considered
λ_n^D	Downlink throughput for UE n
λ_n^U	Uplink throughput for UE n
m_n^D	Number of channels used on the downlink for UE n
m_n^U	Number of channels used by a UE n on the uplink
μ	Average UE spatial density per square meter
N_0	Noise power
N_s	Number of UEs in a sector $s \in \mathcal{B}$
P_{xr}^c	Transmit power on channel c from transmitter x to receiver r
ξ	Pair of uplink and downlink scheduler

local area networks (WLANs), a joint UE association and BSS algorithm is presented in [8]. However, the focus of [8] is only on the downlink transmissions. In [9], a novel antenna beam tilting based dynamic cell expansion technique is proposed for the downlink. The proposed technique is utilized for compensating the coverage loss due to switched off BSs resulting in energy savings. A cell zooming based load balancing and BSS framework is presented in [10]. However, the details of scheduling in uplink/downlink are not discussed. An energy efficient coordinated downlink scheduling for dynamically switching component carrier and BSs based on the variation in load is proposed in [11]. Yet, uplink scheduling and coverage issues are not analysed in [11]. In [12], some of the BSS patterns presented in this work (like $A_{1/3}$ and $A_{3/4}$) are discussed and the amount of energy that can be saved for the various patterns is calculated. However, the actual implementation of BSS, suitable interference model, and the corresponding uplink and downlink scheduling schemes are not discussed. A store-carry-forward relaying based mechanism for energy saving is proposed in [13]. In store-carry-forward relaying, mobile nodes store and carry information messages while in transit and only forward the data as the channel conditions become better. However, suitable scheduling and interference modelling for BSS are not discussed. A dynamic BSS scheme (with load balancing) is proposed in [14] with an exponential

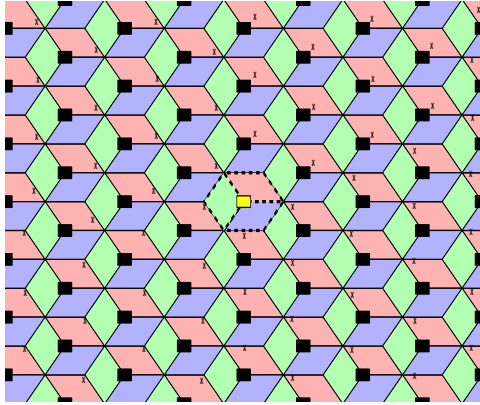


Fig. 1. Nominal system with all BSs are on (the yellow rectangle represents the BS under consideration and 'x' represents location of its uplink interferers).

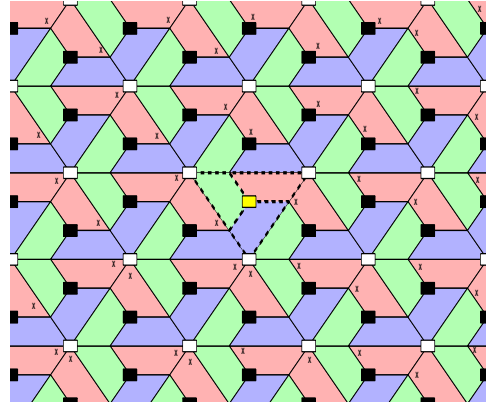


Fig. 2. BSS pattern $A_{2/3}$ with 2 out of 3 BSs are on (the yellow rectangle represents the BS under consideration, white rectangles represent the switched off BSs, and black rectangles represent the BSs still on).

weighted moving average based estimation of the load in the downlink. For computation tractability, average interference estimation for downlink is considered but a similar study for the uplink is required. Results for BSS in a heterogeneous network in a rural environment are presented in [15]. However, in [15], the focus is on the downlink only and it does not consider multiple BSS patterns as presented in this work. The BS activation problem for full coverage on downlink with minimal power consumption in green cellular networks is analysed in [16]. Yet, scheduling and interference modelling are not considered.

Most of the existing work do not deal with the uplink. Any BSS scheme has to be evaluated for both uplink and downlink to ensure that full coverage is maintained even after switching off some BSs. Further, the interference experienced in the system after switching off the BSs must be realistically modeled. This work is a comprehensive study that takes into account the uplink and the downlink focusing on a realistic interference model and flexible scheduling schemes in various cellular environments.

3 SYSTEM MODEL

We consider a homogeneous OFDM-based LTE cellular system composed of B hexagonal cells with sectored macro BSs. Each BS has 3 directional antennas as depicted in Fig. 1. The set of sectors (three per BS) is denoted by $\mathcal{B} = \{1, \dots, 3B\}$. The inter-site distance (ISD) is given (different for urban and rural scenarios).

We consider that at any BS a total of M channels are used with a reuse factor of 3 over the three sectors. Thus, each of the three sectors of a BS is allocated one of the three exclusive bands of $M/3$ channels denoted by \mathcal{M}_1 , \mathcal{M}_2 and \mathcal{M}_3 . We focus on a sector of the BS at the center (let s denote this sector for

the BS represented by the yellow rectangle in Fig. 1). We assume that we have N_s UEs in the sector under consideration (we denote the set of UEs for this sector by \mathcal{N}_s). Assume that this sector uses \mathcal{M}_1 . Further, we assume that the time is divided in frames of T time slots (with \mathcal{T} denoting the set of time slots). We consider a time division duplex (TDD) system such that β proportion of these frames are for the downlink and the rest are for the uplink. We assume that each UE associates with the BS offering the maximum SINR per channel (to be defined) as traditionally done in cellular systems. Finally, the B BSs cover a certain area Δ . The important mathematical notations used in this paper are summarized in Table 1, while the system parameters considered for numerical calculations are presented in Table 3 (more details in Section V).

3.1 BSS Patterns

For mathematical brevity, in the following, we consider a limited number of BSS patterns. However, the framework presented in this paper can be extended to arbitrary number of possible BSS patterns. We investigate the following patterns: $A_{3/4}$ with 3 out of 4 BSs switched on, $A_{2/3}$ with 2 out of 3 BSs switched on, $A_{2/4}$ with 2 out of 4 BSs switched on, $A_{1/3}$ with 1 out of 3 BSs switched on, and $A_{1/4}$ with 1 out of 4 BSs switched on. Thus, a BSS pattern A_{e_1/e_2} is obtained by switching off $(e_2 - e_1)$ BSs out of every e_2 BSs in a predetermined pattern. The nominal system, where all BS are on, is represented by $A_{1/1}$. In Fig. 2, we illustrate BSS pattern $A_{2/3}$ where only the BSs marked by black rectangles are on (i.e., the BSs marked by white rectangles are switched off). Similarly, the pattern $A_{1/3}$ illustrated in Fig. 3, is obtained by switching off all the white BSs. The BSS

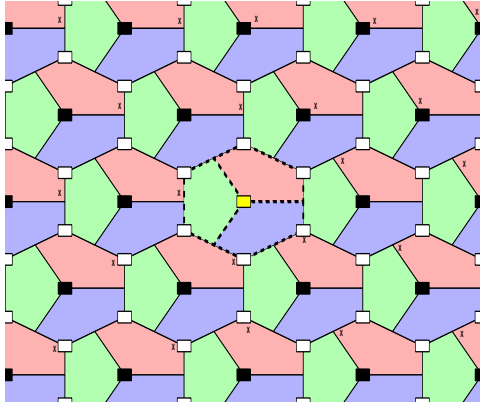


Fig. 3. BSS pattern $A_{1/3}$ with 1 out of 3 BSs are on (the yellow rectangle represents the BS under consideration, white rectangles represent the switched off BSs, and black rectangles represent the BSs still on).

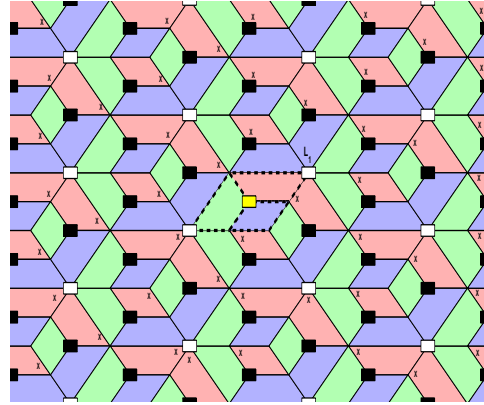


Fig. 4. BSS pattern $A_{3/4}$ with 3 out of 4 BSs are on (the yellow rectangle represents the BS under consideration, white rectangles represent the switched off BSs, and black rectangles represent the BSs still on).

pattern $A_{3/4}$ is illustrated in Fig. 4. For each of the studied patterns, the BSs remaining on have to extend their coverage to compensate for the switched off BSs. The extended coverage for the central BS in the BSS patterns has been depicted in Fig. 2, Fig. 3, and Fig. 4 by the dotted black lines (assuming a constant fading, more details in Section V). For example, the resultant coverage area of the central BS in $A_{2/3}$ becomes a triangle, in $A_{1/3}$ it becomes a bigger rotated hexagon, and in $A_{3/4}$ it becomes a parallelogram. Note that, the coverage area of each sector for any BS (still on) increases with the number of BSs switched off in the predefined BSS patterns. Given a BSS pattern A_{e_1/e_2} , let δ_{e_1/e_2} denote the area of the BS sector under consideration (in m^2). The area of the BS sector is equal to $4/3a$, $3/2a$, and $3a$ for the BSS patterns $A_{3/4}$, $A_{2/3}$, and $A_{1/3}$, respectively, where a is the area of the BS sector in the nominal system $A_{1/1}$. Note that, the sectors of a BS do not remain symmetric for the various BSS patterns, e.g., $A_{3/4}$ has asymmetric sectors as shown for the BS under consideration (yellow rectangle) by the dashed black line in Fig. 4. For BSS patterns with asymmetric sectors, we generate results averaged over all three sectors.

Let the energy consumed per unit time by a BS be denoted by E . Then, $E \times B$ is the energy consumed per unit time by the nominal system, $A_{1/1}$, since all the B BSs are on. Note that the majority of the energy consumption in a typical cellular network is for operating the BSs. Hence, E is approximately constant irrespective of the number of connected UEs [2] (even when no UE is connected with the BS). Thus, a suitable measure of energy efficiency, obtained from a BSS pattern A_{e_1/e_2} is the percentage of energy saving ES_{e_1/e_2} obtained with respect to the nominal system

given by

$$ES_{e_1/e_2} \approx (e_2 - e_1)/e_2 * 100, \quad (1)$$

i.e., if $(e_2 - e_1)$ BSs are switched off out of every e_2 BSs, the total energy savings in the system will be proportional to $(e_2 - e_1)/e_2$.

3.2 User distribution

The UEs are assumed to be randomly distributed in the region Δ with an average UE density of μ per m^2 . Given μ , we define $w(\mu)$ or simply w as a user realization in the area Δ . Then, given a BSS pattern A_{e_1/e_2} and a UE realization w , the number of UEs associated with a sector s is denoted by $N_s(w(\mu), A_{e_1/e_2})$, or simply N_s . Note that the number of users in each sector need not be the same for a given realization and depends on the UEs' distribution. The network is designed for some expected (nominal) user density μ^* . We expect that μ changes over time and falls much below μ^* , for example, at night. In such a case, we investigate whether some BSs can be switched off (using one of the proposed BSS patterns) to save energy while maintaining some level of performance.

3.3 The Channel Model

The SINR from a transmitter x to a receiver r on a channel c is given by

$$\gamma_{xr}^c = P_{xr}^c \frac{G_{xr}^c}{N_0 + I_{xr}^c}, \quad (2)$$

where N_0 is the additive white Gaussian noise power on the channel, G_{xr}^c is the channel gain between x and r on c , P_{xr}^c is the transmit power used by x and I_{xr}^c is the cumulative interference seen by the receiver r on channel c . Note that P_{xr}^c is allocated by the

scheduler and that the interference $I_{x_r}^c$ is a function of the locations of the interferers (which depends on the BSS pattern), and the transmit power they use on c which is in turn a function of the scheduler.

We consider symmetric uplink and downlink channel gains. Given a user realization w , we assume that the BS has the knowledge of UEs' channel gains and an estimate of the interference. Further, we assume that the interfering BSs use the same scheduling schemes as the BS under consideration on both uplink and downlink. The interferers on a downlink are the BSs transmitting on the same band and their positions are known and fixed. Unlike the downlink, the interfering UE locations for the uplink are not fixed and known. Given a BSS pattern, to simplify the analysis, we consider the interfering UE locations (one per sector sharing the same channels as the sector under consideration) to be such that they yield high interference to any point in the sector (i.e., in Fig 1, Fig. 2, Fig. 3, and Fig. 4, "x" represents the locations of all the uplink interferers for a UE in the "pink" sector of the BS at the centre, marked by a yellow rectangle). *In summary, the SINR is a function of the transmit power per channel and the interference that significantly depend on the scheduler for both the uplink and the downlink.* Further, the interference also depends on the BSS pattern.

3.4 Scheduling

Scheduling is the core functionality of a cellular network in that it affects performance and interference. There are many ways to design a scheduler (be it on the downlink or the uplink). A scheduler allocates a combination of channels, power per channel, and time slots to each UE to optimize an objective function. Typically, to provide proportional fairness to UEs [3], the objective is to maximize the product of the UEs' throughput assuming that each UE is greedy. By allocating in a (downlink or uplink) frame, power to channels and channel to UEs on a time slot basis, a scheduler allocates a specific per frame throughput to a UE and this allocation produces inter-sector interference. The resources to be allocated to the UEs associated to the BS are different for the downlink and uplink. In the downlink, the BS transmit power is distributed over the channels in each time slot, while in the uplink, each UE brings its own power P_{UE} . The difficulty with scheduling comes from the fact that it has to be computed often, fast, and it is intractable in its most generic form. Hence, the objective is to design schedulers that are tractable and quasi-optimal. The problem has received a lot of attention for a nominal (i.e., $A_{1/1}$) system on the downlink but little attention in the case of BSS where flexibility becomes another criteria as we will see next. We denote a pair of scheduling schemes by $\xi = (\xi^D, \xi^U)$, where ξ^D and ξ^U denote the downlink and uplink schedulers, respectively.

3.5 Coverage

We define coverage with respect to a non-zero rate. The rate that a UE receives on the downlink (resp. the uplink) depends on the downlink (resp. the uplink) scheduler, its channel gains, the BSS pattern under consideration, and the resultant interference. In the following, we say that a scheduler ξ^D (resp. ξ^U) provides full coverage in the downlink (resp. uplink) if the scheduler can provide non-zero rate to the UE at the farthest locations (a function of the BSS pattern) as long as the fading is less than a certain predetermined threshold.

3.6 Performance Metric

Let $\lambda_n^D(\xi^D, w, A_{e1/e2})$ and $\lambda_n^U(\xi^U, w, A_{e1/e2})$, respectively, denote the downlink and the uplink throughput of a UE n for a given realization w , a scheduler pair (ξ^D, ξ^U) , and a BSS pattern $A_{e1/e2}$. Note that $\lambda_n^D(\xi^D, w, A_{e1/e2})$ (resp. $\lambda_n^U(\xi^U, w, A_{e1/e2})$) depends significantly on the scheduler ξ^D (resp. ξ^U) and the BSS pattern under consideration. We consider the geometric mean throughput of all the UEs in the sector of the cell under consideration as our metric for quantifying user performance (this is the natural metric if we consider proportional fairness as the fairness criteria [15], [17]). We denote the geometric mean throughput of the UEs in the sector on the downlink and uplink by $GM_s^D(\xi^D, w, A_{e1/e2})$ and by $GM_s^U(\xi^U, w, A_{e1/e2})$, respectively. Then, we have

$$GM_s^D(\xi^D, w, A_{e1/e2}) = \sqrt[N_s]{\prod_{n=1}^{N_s} \lambda_n^D(\xi^D, w, A_{e1/e2})},$$

$$GM_s^U(\xi^U, w, A_{e1/e2}) = \sqrt[N_s]{\prod_{n=1}^{N_s} \lambda_n^U(\xi^U, w, A_{e1/e2})}. \quad (3)$$

where N_s is the number of UE connected to the sector for the realization w and the BSS pattern $A_{e1/e2}$. We then define the overall performance metric of a sector for a given w , $A_{e1/e2}$, and a scheduler pair ξ as

$$\Gamma_s(\xi, w, A_{e1/e2}) \triangleq GM_s^D(\xi^D, w, A_{e1/e2}) + GM_s^U(\xi^U, w, A_{e1/e2}). \quad (4)$$

We have already shown that the BS sectors need not be symmetric for the various BSS patterns. Hence, for a scheduler pair ξ , a user density μ , and a BSS pattern $A_{e1/e2}$, the cell level average performance metric is defined, using (5), as

$$\Gamma(\xi, \mu, A_{e1/e2}) \triangleq E_w \left[\frac{1}{3} \sum_{s \in \mathcal{S}} \Gamma_s(\xi, w, A_{e1/e2}) \right], \quad (5)$$

where the expectation is over the UE realizations w and \mathcal{S} represents the set of sectors associated with the cell under consideration. Although, the BS sectors may not be symmetric, all the cells of a BSS pattern

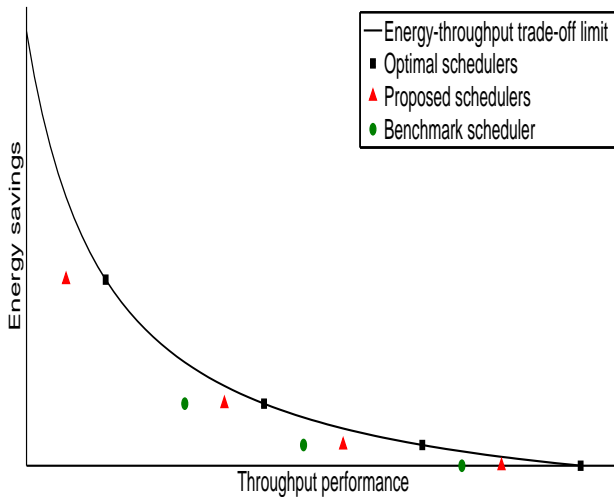


Fig. 5. Energy savings versus throughput trade-off for a given user density.

have the same coverage area. Hence, the extension of the performance results from a cell to a system level is trivial and not considered. Next, we present the theoretical formulation of the problem considered in this paper.

3.7 Problem Formulation

Our design objective is to maximize the system performance metric (given in (5)) for each BSS pattern. Note that we have already shown the computation of energy savings from a BSS pattern in (1). Given a user density μ , a scheduler pair ξ , a TDD time fraction β , and a finite set of BSS patterns, we will obtain energy savings versus throughput performance trade-off curves as a set of possible points (represented in Fig. 5 by one point per BSS pattern and a scheduler pair) instead of a continuous energy-performance Pareto frontier described in [7] (depicted by the throughput-energy trade-off limit in Fig. 5). Further, it is possible that the optimal scheduler pair can provide full coverage for a given BSS pattern while it is not so for another pair (e.g., there is no green circle for the highest energy saving in Fig. 5). Hence, for any specific scheduler pair there might exist BSS patterns for which full coverage cannot be provided, such patterns are considered as unfeasible. Thus, the design objective for a feasible BSS pattern, can be represented as a maximization of (5) for a given ξ , μ , and $A_{e1/e2}$. Note that we will obtain different sets of trade-off points depending on the schedulers. The optimal schedulers for uplink and downlink can reach the trade-off limit as depicted in Fig. 5. However, as will be shown later, optimal schedulers can be computationally complex and not usable in a realistic scenario. Hence, our objective is to propose suitable uplink and downlink schedulers that can deliver good throughput-energy trade-offs compared to the existing benchmark schedulers (discussed later). In the

next section, we present the different downlink and uplink schedulers considered in this paper for BSS.

4 SCHEDULING FOR BSS

Given a BSS pattern $A_{e1/e2}$, a TDD time fraction β , and a user realization w in the sector under consideration, we consider various scheduling schemes in this section. Note that given β and a scheduler pair ξ , using (5), we can completely decouple the performance metric per sector $\Gamma_s(\xi, w, A_{e1/e2})$ for the downlink and the uplink. We first consider the case of optimal schedulers on the downlink and the uplink.

4.1 Optimal Schedulers

On the downlink, the optimal scheduler in a sector will allocate, in every downlink frame, the available channels ($M/3$) and the time slots (T) to the UEs with the BS transmit power ($P_{BS}/3$) suitably distributed over the channels in each time slot. Given the number of UEs in the sector N_s , the optimal downlink scheduling at this sector can be formulated as the following optimization problem ξ_{opti}^D

$$\xi_{opti}^D : \max_{\{x_n^{t,c}\}, \{P_n^{t,c}\}} \left(\prod_{n \in \mathcal{N}_s} \lambda_n^D(\xi_{opti}^D, w, A_{e1/e2}) \right) \quad (6)$$

$$\text{s.t. } x_n^{t,c} \in \{0, 1\} \forall t \in \mathcal{T}, c \in \mathcal{M}_1, n \in \mathcal{N}_s, \quad (7)$$

$$\sum_{n \in \mathcal{N}_s} \sum_{c \in \mathcal{M}_1} P_n^{t,c} \leq \frac{P_{BS}}{3} \forall t \in \mathcal{T}, \quad (8)$$

$$\sum_{n \in \mathcal{N}_s} x_n^{t,c} \leq 1 \forall t \in \mathcal{T}, c \in \mathcal{M}_1, \quad (9)$$

$$P_n^{t,c} \leq \frac{x_n^{t,c} P_{BS}}{3} \forall t \in \mathcal{T}, c \in \mathcal{M}_1, n \in \mathcal{N}_s, \quad (10)$$

$$\lambda_n^D(\xi_{opti}^D, w, A_{e1/e2}) = \sum_{t \in \mathcal{T}} \sum_{c \in \mathcal{M}_1} \beta x_n^{t,c} f\left(\frac{P_n^{t,c} G_{sn}^c}{N_0 + I_{sn}^{t,c}}\right) \forall n \in \mathcal{N}_s, \quad (11)$$

where f is a mapping between the SINR per channel and the efficiency of the modulation and coding scheme (MCS) for LTE given in Table 2, $P_n^{t,c}$ denotes the downlink transmit power from the BS sector s to UE n in time slot t and channel c . The interference at UE n in time slot t on channel c can be calculated as follows

$$I_{sn}^{t,c} = \left(\sum_{\hat{s} \neq s, \hat{s} \in \mathcal{B}} P_{\hat{s}}^{t,c} G_{\hat{s}n}^c \right), \quad (12)$$

where, $P_{\hat{s}}^{t,c}$ is the downlink power allocated by the scheduler at the interfering BS \hat{s} on the same channel c (equal to zero if the channel is not in use or the BS is switched off in the BSS pattern under consideration), $G_{\hat{s}n}^c$ is the channel gain from the BS \hat{s} to the UE (for the sectors using the same channels as the one under consideration), and the location of the interferers are known. We assume adaptive modulations with discrete rates such that whenever the SINR lies between any two thresholds, in Table 2, the rate $f(P_n^{t,c} G_{sn}^c / (N_0 + I_{sn}^{t,c}))$ obtained by the UE on that channel is the corresponding efficiency multiplied with $SC_{OFDM} SY_{OFDM} / T_{subframe}$ [18]. Similarly, given N_s , the optimal uplink scheduling at a

TABLE 2
Modulation and Coding Schemes-LTE

SINR thresholds (in dB)	-6.5	-4	-2.6	-1	1	3	6.6	10	11.4	11.8	13	13.8	15.6	16.8	17.6
Efficiency (in bits/symbol)	0.15	0.23	0.38	0.60	0.88	1.18	1.48	1.91	2.41	2.73	3.32	3.9	4.52	5.12	5.55

sector can be formulated as the following optimization problem ξ_{opti}^U ,

$$\xi_{\text{opti}}^U : \max_{\{x_n^{t,c}\}, \{P_n^{t,c}\}} \left(\prod_{n \in \mathcal{N}_s} \lambda_n^U(\xi_{\text{opti}}^U, w, A_{e1/e2}) \right) \quad (13)$$

$$\text{s.t. } x_n^{t,c} \in [0, 1] \forall t \in \mathcal{T}, c \in \mathcal{M}_1, n \in \mathcal{N}_s, \quad (14)$$

$$\sum_{c \in \mathcal{M}_1} P_n^{t,c} \leq P_{UE} \forall t \in \mathcal{T}, n \in \mathcal{N}_s, \quad (15)$$

$$\sum_{n \in \mathcal{N}_s} x_n^{t,c} \leq 1 \forall t \in \mathcal{T}, c \in \mathcal{M}_1, \quad (16)$$

$$P_n^{t,c} \leq x_n^{t,c} P_{UE} \forall t \in \mathcal{T}, c \in \mathcal{M}_1, n \in \mathcal{N}_s, \quad (17)$$

$$\lambda_n^U(\xi_{\text{opti}}^U, w, A_{e1/e2}) = \sum_{t \in \mathcal{T}} \sum_{c \in \mathcal{M}_1} (1-\beta) x_n^{t,c} f\left(\frac{P_n^{t,c} G_{sn}^c}{N_0 + I_{ns}^{t,c}}\right) \forall n \in \mathcal{N}_s, \quad (18)$$

where $I_{ns}^{t,c}$ represents the interference on channel c seen by the BS due to UEs other than UE n operating on the same channel in the nearby cell sectors (represented by an expression similar to (12)) at time t and is a function of the BSS pattern and the scheduling at each of the interfering BSs.

Given the optimal downlink and uplink scheduling schemes in (6) and (13), we can compute the performance metric (in (5)) by averaging over multiple UE realizations and the sectors of the BS under consideration for a BSS pattern and β . However, the optimal schedulers for the downlink and the uplink described in (6) and (13), respectively, have non-linear objective functions, non-linear constraints, and integer variables. Moreover, the interference in the SINR ((11) and (18)) is dependent on the scheduling at the interfering sectors as well as the BSS pattern and is difficult to estimate. Thus, the optimization problems ξ_{opti}^D and ξ_{opti}^U are NP-hard and difficult to solve for a practical cellular network. This has motivated the proposal of simpler schedulers that we call benchmark schedulers and present in the following sub-section. They were proposed in the context of nominal systems (i.e., $A_{1/1}$) because they provide full coverage, are simple in terms of power allocation, and make the estimation of the interference relatively easy. The problem is that they do not fare well in the BSS context.

4.2 Benchmark Schedulers

For mathematical brevity, in the rest of the paper, we assume that the channels are flat. The downlink scheduler assumes that the BS allocates all its power ($P_{BS}/3$ in each sector) to a UE n in a given time slot. This single-UE scheduling in a downlink time slot is a strong but natural assumption due to the coupling of power in the downlink. It enables the simplification

of the problem especially if we relax the integrality of time. Let α_n^D denote the fraction of the downlink time the BS allocates to UE n . During this fraction of time, the sector's transmit power is used only to transmit to UE n . This power is then equally divided over all the $M/3$ channels. Thus, the benchmark downlink scheduler ξ_{bench}^D can be represented as the following optimization problem.

$$\xi_{\text{bench}}^D : \max_{\{\alpha_n^D\}} \left(\prod_{n \in \mathcal{N}_s} \lambda_n^D(\xi_{\text{bench}}^D, w, A_{e1/e2}) \right) \quad (19)$$

$$\text{s.t. } \sum_{n \in \mathcal{N}_s} \alpha_n^D = \beta, \quad (20)$$

$$\lambda_n^D(\xi_{\text{bench}}^D, w, A_{e1/e2}) = \frac{M\alpha_n^D}{3} f\left(\frac{P_{BS} G_{sn}^c}{M N_0 + I_{sn}^c}\right) \forall n \in \mathcal{N}_s. \quad (21)$$

It has been shown in [17] that this proportional fair scheduler will allocate equal fraction of time to all UEs. Hence, on the downlink, the benchmark scheduler allocates, to each UE in the sector, $M/3$ channels for β/N_s fraction of the time and transmits with equal power per channel $P_n^{D,c} = P_{BS}/M$ on any channel $c \in \mathcal{M}_1$. Further, interference is easy to compute for the benchmark scheduler as the neighboring BSs are also transmitting at a known power at any time on each channel.

In the uplink, the benchmark scheduler ξ_{bench}^U allocates to each UE n in the sector $M/(3N_s)$ channels for the complete uplink $(1-\beta)$ fraction of time². Further, we assume that a UE uses its transmit power P_{UE} equally over the $M/(3N_s)$ channels.

These schedulers work well in a nominal system (both in an urban and rural environments). However, when switching off some BSs to save energy (i.e., for all the BSS patterns), situations can arise where distributing power equally on all the channels for the downlink (and allocating a fixed number of channels on the uplink) can result in coverage holes (by spreading the power too thin). For example, given a rural macro-cell environment, let us assume the system is in BSS pattern $A_{3/4}$. Consider a UE close to the centre of the switched off white BS marked by L_1 in Fig. 4. This UE in Fig. 4 is approximately at a distance of 1732 m from the closest BS still on. Assuming that 5 users per sector are present and a total of 30 channels ($M/3$) are available in the

2. For mathematical brevity, we assume $M/(3N_s)$ to be a positive integer. We can equally consider, without any loss of generality, $\Omega = \text{mod}(M/3, N_s)$ users are allocated $\lfloor M/(3N_s) \rfloor + 1$ channels, whereas, $N_s - \Omega$ users get $\lfloor M/(3N_s) \rfloor$ channels as given in [3].

extended sector, then the benchmark scheduler will allocate 6 channels ($M/(3 \times 5)$) to each user for uplink. Using Table 3 (more explanation on Table 3 will be given in the numerical results section), the SINR per channel of the UE at L_1 will be approximately -9 dB. This value is much lower than the minimum SINR threshold (-6.5 dB) given in Table 2 resulting in a coverage hole at L_1 . Similarly, it can be shown that the location L_1 is not covered by the benchmark uplink scheduler for any of the proposed BSS patterns. The situation worsens with a decrease in the number of UEs per sector as the power per channel on the uplink decreases with N_s for the benchmark scheduler (recall that $P_n^{U,c} = 3P_{UE}N_s/M$). Using the benchmark uplink scheduler for the BSS patterns $A_{3/4}$, $A_{2/3}$, and $A_{1/3}$ result in a coverage loss of approximately 10%, 5%, and 15%, respectively. Thus, to ensure full coverage, a new uplink scheduler is needed, one that allows power to be focused on appropriate number of channels. Note that coverage holes on the downlink due to the benchmark downlink scheduler do exist but are less significant. This means that a new (more flexible) downlink scheduler is also needed.

4.3 Proposed Schedulers

We will design our schedulers using the insight described below. Given a transmitter, a receiver, and the discrete rate function in Table 2, spreading all the transmit power over all the available channels is not always an optimal strategy from the perspective of user performance. To illustrate this, we consider a transmitter at a fixed location and a receiver that can be at five different locations, each one yielding a SNR (we assume no interference for the purpose of this illustration) when the transmit power is focused on one channel equal to 3 dB, 6.6 dB, 10 dB, 13 dB, and 17.6 dB, respectively. We compute the rates (see Fig. 6) that the receiver would obtain at these five locations if the transmitter were forced to transmit over exactly $m \leq M$ channels. We also include in Fig. 6 the theoretical rate obtained by considering the logarithmic rate model, typically, considered in the literature for one of the locations. For the logarithmic rate model, spreading power on more channels always increases performance (i.e., the data rate at the receiver). However, this is not true for the discrete rate model. Fig. 6 shows that for some of the locations (corresponding to very low SNR) spreading the power on many channels results in zero rate (i.e., no coverage). But even for the locations with higher SNR, Fig. 6 indicates that a higher rate is achievable by using less than $M = 33$ channels.

For example, for the BSS patterns $A_{3/4}$, $A_{2/3}$, and $A_{1/3}$, the percentage of locations where uplink users can obtain higher throughput by utilizing less channels than the benchmark scheduler allocates is 51%, 48%, and 63% for a nominal 15 users in the cell, in

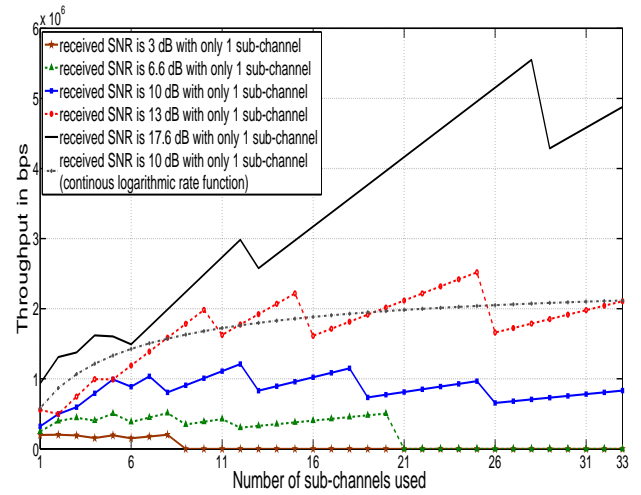


Fig. 6. Rate obtained at different locations as a function of the number of channels used by the transmitter.

a rural macro-cell environment. Hence, the BS must select the number of channels on which to transmit for both downlink and uplink carefully to ensure better performance and full coverage. This motivates our proposed downlink and uplink schedulers in which power can be focused on a lower number of channels to ensure higher throughput and full coverage.

Our proposed scheduling schemes for downlink and uplink are generalizations of the benchmark ones. The goal of the proposed schemes is to provide more flexibility in terms of power allocation. We keep the principle of sharing the downlink equally in time between the UEs, i.e., $\alpha_n^D = \beta/N_s$ and dedicate all the BS transmit power in a sector, i.e., $P_{BS}/3$, to a UE at a time. However, we allow the BS to spread this power over less than $M/3$ channels, i.e., we allow the BS to focus its power on $m_n^D \leq M/3$ channels for UE n . Additionally, to keep the interference manageable, we do not allow the BS to focus the power on strictly less than X channels (where X is a system parameter and its selection is discussed in the next section). Thus, we can represent our downlink scheduler as an optimization problem given by

$$\xi_{prop}^D : \max_{\{m_n^D\}} \prod_{n \in \mathcal{N}_s} \lambda_n^D(\xi_{prop}^D, w, A_{e1/e2}) \quad (22)$$

$$\text{s.t. } X \leq m_n^D \leq \frac{M}{3}, m_n^D \in \mathbb{N}, \forall n \in \mathcal{N}_s, \quad (23)$$

$$P_n^{D,c} = \frac{P_{BS}}{3m_n^D} \text{ for } m_n^D \text{ channels,} \quad (24)$$

$$= 0 \text{ for } \left(\frac{M}{3} - m_n^D\right) \text{ channels,}$$

$$\lambda_n^D(\xi_{prop}^D, w, A_{e1/e2}) = \frac{m_n^D \beta}{N_s} f\left(\frac{P_n^{D,c} G_{sn}^c}{N_0 + I_{sn}^c}\right) \forall n \in \mathcal{N}_s, \quad (25)$$

where the interference can be upper bounded by

$$I_{sn}^c \leq \left(\sum_{\hat{s} \neq s, \hat{s} \in \mathcal{B}} \frac{P_{BS} G_{\hat{s}n}^c}{3X} \right). \quad (26)$$

By lower bounding the number of channels that can be allocated to a UE on the downlink by X , we ensure

that the worst case interference on the downlink is bounded by a function of $P_{BS}/(3X)$ as shown in (26), i.e., we make sure that all BSs use no more than $P_{BS}/(3X)$ on any channel. Note that by focusing the power on less channels, we increase the interference that the neighboring BSs generate on some channels, while we decrease their interference on the other channels (not used). By not taking into account the fact that some channels can be better off, we are in fact computing a lower bound on the possible throughput. Note that as the BS uses the whole power for one UE, the unused channels cannot be used for other UEs (no power is left for the downlink to use at the same time). Thus, for a given predetermined value of X , we can decouple the problem in (22) and separately optimize λ_n^D for each UE in its allocated fraction of time as the following optimization problem $\Phi(n, w, A_{e1/e2})$,

$$\Phi(n, w, A_{e1/e2}) : \max_{m_n^D} \lambda_n^D(\xi_{prop}^D, w, A_{e1/e2}) \quad (27)$$

$$\text{s.t. } X \leq m_n^D \leq \frac{M}{3}, m_n^D \in \mathbb{N}, \quad (28)$$

$$P_n^{D,c} = \frac{P_{BS}}{3m_n^D} \text{ for } m_n^D \text{ channels,} \quad (29)$$

$$= 0 \text{ for } \left(\frac{M}{3} - m_n^D\right) \text{ channels,}$$

$$\lambda_n^D(\xi_{prop}^D, w, A_{e1/e2}) = \frac{m_n^D \beta}{N_s} f\left(\frac{P_n^{D,c} G_{sn}^c}{N_0 + I_{sn}^c}\right), \quad (30)$$

The optimization problem in (27) gives the number of channels to be used for the given UE on the downlink. Note that the benchmark downlink scheduler is a feasible solution of the scheduler proposed above as long as there is coverage.

Now, we focus on the uplink. We keep the principle that a UE is allocated a set of channels at all time the uplink is on, i.e., $(1-\beta)$ of the time, but the cardinality of this set is computed on a per realization basis (i.e., depending on the number of UEs and their locations) to make sure that each UE spreads its transmit power more efficiently. The UE transmit power is equally allocated to all channels in the set. Further, we assume that a UE cannot be allocated less than Y channels (to upper bound the interference). The proposed uplink scheduler corresponds to the following problem:

$$\xi_{prop}^U : \max_{\{m_n^U\}} \prod_{n \in \mathcal{N}_s} \lambda_n^U(\xi_{prop}^U, w, A_{e1/e2}) \quad (31)$$

$$\text{s.t. } \sum_{n \in \mathcal{N}_s} m_n^U \leq \frac{M}{3}, m_n^U \in \mathbb{N}, m_n^U \geq Y \forall n \in \mathcal{N}_s, \quad (32)$$

$$P_n^{U,c} = \frac{P_{UE}}{m_n^U} \text{ for } m_n^U \text{ channels,} \quad (33)$$

$$= 0 \text{ for } \left(\frac{M}{3} - m_n^U\right) \text{ channels,}$$

$$\lambda_n^U(\xi_{prop}^U, w, A_{e1/e2}) = m_n^U (1-\beta) f\left(\frac{P_n^{U,c} G_{sn}^c}{N_0 + I_{ns}^c}\right) \forall n \in \mathcal{N}_s \quad (34)$$

where the interference can be upper bounded by

$$I_{ns}^c \leq \left(\sum_{\hat{n} \neq n} \frac{P_{UE} G_{s\hat{n}}^c}{Y} \right). \quad (35)$$

The upper bound in (35) is a conservative estimate of the uplink interference as the interfering UEs in

the neighboring cells may be spreading their power on more than Y channels. Note that the benchmark uplink scheduler is a feasible solution of this proposed scheme as long as there is coverage. Unlike the downlink scheduler, the proposed uplink scheduler cannot be decoupled on a per UE basis.

The proposed schedulers are more flexible than the benchmark schedulers when BSs are switched off since the transmit power can be focused on the right number of channels to ensure coverage over larger distance (in BSS). The results obtained from (22) (resp. (31)) depend on selecting the appropriate value of X for the downlink (resp. Y for the uplink). For a given BSS pattern, the same predetermined values of X and Y should be used by all the BSs else whenever an active BS changes its X and Y this information has to be exchanged since this would affect the interference produced by the sector. Thus, to save this overhead in information transmission, we present an off-line approach for calculating a common value for X and one for Y for all the BSs for each of the BSS patterns.

4.4 Computation of X and Y for a given BSS pattern

The lower the value of X (resp. Y), the more flexibility the downlink (resp. uplink) scheduling scheme has to adjust the number of channels allocated to each UE but the higher the price in terms of interference. If X (resp. Y) is too large, it is possible that a given BSS pattern cannot offer full coverage. Hence, we first compute for a given BSS pattern $A_{e1/e2}$ the set $\mathcal{X}_{e1/e2}$ (resp. $\mathcal{Y}_{e1/e2}$) of values of X (resp. Y) enabling full coverage on the downlink (resp. on the uplink). Then, we select, for a given user density, the values of X in $\mathcal{X}_{e1/e2}$ and Y in $\mathcal{Y}_{e1/e2}$ such that the geometric mean throughput (averaged over the user realizations w) in the downlink and the uplink are maximized, respectively.

Previously, it was shown that the proposed downlink scheduler can be decoupled to a maximization problem per UE (given a UE location). Thus, for any BSS pattern, in the downlink, we select the value of X which maximizes, for a given user density, the per user geometric mean throughput averaged over UE realizations in a sector. Further, if the sectors of the extended BS coverage are not symmetric (for example, in $A_{2/4}$ and $A_{3/4}$), we average over all the sectors in the cell. Then, $X_{e1/e2}$ is selected such that

$$X_{e1/e2} = \arg \max_{X \in \mathcal{X}_{e1/e2}} E_w[\Phi(n)], \quad (36)$$

where $\Phi(n)$ represents the optimization problem in (27). Note that, in (36), we solve $\Phi(n)$ for all feasible values of X , i.e., for all values of $X \in \mathcal{X}_{e1/e2}$, that ensure full coverage for the BSS pattern $A_{e1/e2}$. The value of $X \in \mathcal{X}_{e1/e2}$ that maximizes the expected value of the objective is selected. We denote this value by $X_{e1/e2}$. Thus, an operator can solve (27) a priori

TABLE 3
System parameters

Noise power	-174 $\frac{dBm}{Hz}$	P^{BS}	46 dBm
Noise figure	5 dB	P^{UE}	24 dBm
BS antenna gain G_a	17 dBi	SC_{OFDM}	12
UE antenna gain	0 dBi	SY_{OFDM}	14
channel bandwidth	180 KHz	$\zeta_{l,b}^m$	20 dBm
carrier frequency	800 MHz	ν^{RURAL}	9 dB
M	99	ν^{URBAN}	20 dB
ISD^{RURAL}	1732 m	ISD^{URBAN}	500 m
$PL_{l,b}(d)^{RURAL} = 117.5953 + 38.6334 \log_{10}(d/1000), d \geq 35$			
$PL_{l,b}(d)^{URBAN} = 128 + 37.6 \log_{10}(d/1000), d \geq 35$			

Algorithm 4.1: UPLINK SCHEDULING HEURISTIC(.)

INPUTS: $\{\psi_n\}$, M , N_s , and $Y_{e1/e2}$

OUTPUTS: $\{\lambda_n^U\}$ and $\{m_n^U\}$

-
- 1: Initialize: $n = 1$, $\chi = M/3$, and $\tau = N_s$
 - 2: Sort array $\{\psi_n\}$ in increasing order
 - 3: **Repeat**
 - 4: Set $m_n = Y_{e1/e2}$, $m_n^U = Y_{e1/e2}$, and $\lambda_n^U = 0$
 - 5: **Repeat**
 - 6: Compute $\lambda(m_n, (P_{UE}/m_n) \times \psi_n)$ as in (34)
 - 7: **If** $\lambda(m_n, (P_{UE}/m_n) \times \psi_n) > \lambda_n^U$
 - {Set $m_n^U = m_n$ and
 - $\lambda_n^U = \lambda(m_n, (P_{UE}/m_n) \times \psi_n)$
 - End**
 - 8: Set $\chi = \chi - m_n^U$, $\tau = \tau - 1$, and $m_n = m_n + 1$
 - 9: **Until** $m_n \geq \lfloor \chi/\tau \rfloor + 1$
 - 10: Set $n = n + 1$
 - 11: **Until** $n \geq N_s + 1$

for all feasible values of X , average over various possible UE realizations, and select the value $X_{e1/e2}$ that results in the maximum objective in an average sense. This predetermined value of $X_{e1/e2}$ is then used at each BS for scheduling through (27).

Given the spatial probability distribution function (PDF) for the UEs and the PDF for channel fading in the system, the problem in (36) can be solved by averaging over various possible realizations of G_{sn}^c . For the specific case of uniformly distributed UEs, the problem can be further simplified as will be shown in the numerical result section. Selecting the value of X in the manner described above will ensure that all UEs will be covered and the average geometric mean throughput will be maximized for a given BSS pattern.

When the BSs are switched off, the situation on the uplink is quite different from the downlink. Our numerical results have shown that for patterns $A_{1/3}$, $A_{2/3}$, and $A_{3/4}$, the only value of Y that ensures full coverage in urban as well as rural macro-cell environment is 1. For any value of Y higher than 1, coverage holes exist in the system.

4.5 Computational Complexity and Heuristic

The proposed downlink scheduler is easily decoupled to a maximization problem per UE as shown in (27). Given the user location/channel gains, the problem in (27) is to evaluate the user throughput for all possible values of m_n^D . Hence, it has a complexity of the order of $\mathcal{O}(M)$. To solve the downlink scheduling problem, i.e., (22), the problem in (27) has to be evaluated for all N_s users. Thus, the downlink scheduler in (22) has a relatively low complexity of the order of $\mathcal{O}(MN_s)$.

The uplink scheduling scheme given in (31) cannot be decoupled to a per UE basis. Further, the problem is a mixed integer non-linear program (MINLP). Such problems, in general, are difficult to solve and have a high complexity. Hence, we present a heuristic which can be used to approximately solve (31) with significantly lower computational cost. Given that the BS has the knowledge of the UEs' channel gains and the interference, it can easily compute an estimate of $\psi_n = G_{sn}^c / (N_0 + I_{ns}^c)$ for all n UEs. Note that ψ_n is a function of the BSS pattern $A_{e1/e2}$ and the UE realization w . The BS can sort this array $\{\psi_n\}$ in increasing order with a complexity order equal to $\mathcal{O}(N_s \log N_s)$. Given this sorted array, the BS focuses on the UE with the worst ψ_n and computes the optimal number of channels (by dividing the total transmit power P_{UE} on these channels and calculating the resultant rate) from the set $\{Y_{e1/e2}, \dots, \lfloor M/(3N_s) \rfloor\}$, where $Y_{e1/e2}$ is selected as explained in the previous subsection to ensure full coverage. Then, the BS focuses on the second worst-off UE (with the second lowest ψ_n) and computes the optimal number of channels from the set ranging from $Y_{e1/e2}$ to $\chi/\tau = \lfloor \text{total number of remaining channels} / \text{the remaining number of UEs} \rfloor$. This process is repeated till all the UEs have been allocated channels. The complexity order of this part of the heuristic (beyond the sorting) is $\mathcal{O}(MN_s)$. Hence, the overall complexity order of the proposed heuristic is $\mathcal{O}(N_s \log N_s + MN_s)$ which is very low.

A pseudo-code for the above heuristic is presented in Algorithm 4.1. We will validate it with respect to the proposed uplink scheduler in the next section where we present numerical results for various realistic LTE cellular settings and some engineering insights based on these results.

5 NUMERICAL RESULTS

We consider a system composed of 77 macro-cells as depicted in Fig. 1. We study the user performance in the "pink" sector of the central macro-cell marked by a yellow rectangle in Fig. 1 on both the uplink and the downlink for different BSS patterns. Typically, uniform distribution of UEs has been recommended for simulating the LTE macro-cell environment [3].

Hence, we consider an average user density in the range of 1 to 5 users per km^2 , i.e., close to 1 to 15 users per $2.598 \times 10^6 \text{ m}^2$ (the area of a rural macro-cell in the nominal system). To study the relative impact in the urban macro-cell area, we consider 4 to 68 users per km^2 , i.e., of the order of 1 to 15 users per $2.165 \times 10^5 \text{ m}^2$ (the area of an urban macro-cell in the nominal system). We consider the nominal system and the BSS patterns $A_{3/4}$, $A_{2/3}$, and $A_{1/3}$. We also consider BSS patterns $A_{2/4}$ and $A_{1/4}$. However, they do not offer full coverage for the considered fading (see later). We divide the total area under consideration Δ into a $\kappa_1 \times \kappa_2$ grid and assume that UEs can only be positioned at one of the points on the grid. In the nominal system, with all the BSs turned on, the coverage area of each sector for any BS contains L such positions. Thus, given a BSS pattern, a user can be at any location l , $l \in \mathcal{L}_{e_1/e_2}$, with equal probability. The ISD of the macro-cells is considered to be 500 and 1732 m for the urban and rural environments, respectively. For the rural macro-cell environment, the UEs are positioned on a 15588×14000 grid with a spacing of 10 m resulting in $L = 5800$ locations per sector for the nominal system. Whereas, in case of the urban macro-cell, due to reduced ISD, we consider 4500×4000 grid with $L = 484$ locations per sector for the nominal scenario. For each of these BSS patterns and a given user density, we generate 200 random realizations of the UE locations.

To calculate the SINR per channel (2) for a UE n at location l , i.e., $\gamma_{sn}^c(l)$ and $\gamma_{ns}^c(l)$, for uplink and downlink, respectively, we consider the following calculations. Given log normal shadowing, the channel gain for a UE n at any location l with respect to sector s , $s \in \mathcal{B}$, on any channel c is denoted by $G_{sn}^c(l)$, such that

$$G_{sn}^c(l) = D_{l,b}(\theta) \times G_a \times \zeta_{l,b}^c \times \nu \times PL_{l,b}(d), \quad (37)$$

where $D_{l,b}(\theta) = -\min \left\{ 12 \left(\frac{\theta}{70^\circ} \right)^2, 20 \right\}$ dB represents the directivity gain with θ being the angle made by the location l with the broadside direction of the antenna from a BS sector s [3], G_a consists of the antenna gains, $\zeta_{l,b}^c$ denotes the slow fading on the channel, ν is the penetration loss, and $PL_{l,b}(d)$ is the path loss with d being the distance between location l and BS sector s . Note that the ISD, $PL_{l,b}(d)$, and ν are different for urban and rural macro-cell environments. Suitable additional details of the physical layer parameters used in our computations are given in Table 3. We assume a constant fading loss equal to 2.5 times the typical standard deviation of fading (8 dB), i.e., $\zeta_{l,b}^c$ is equal to 20 dB. More precisely, considering this high fading ensures a sufficient fading margin such that more than 99% of the possible fading realizations result in non-zero rates. This is in coherence with our definition of coverage where the threshold is set to a high value. The UE and BS transmit powers are taken

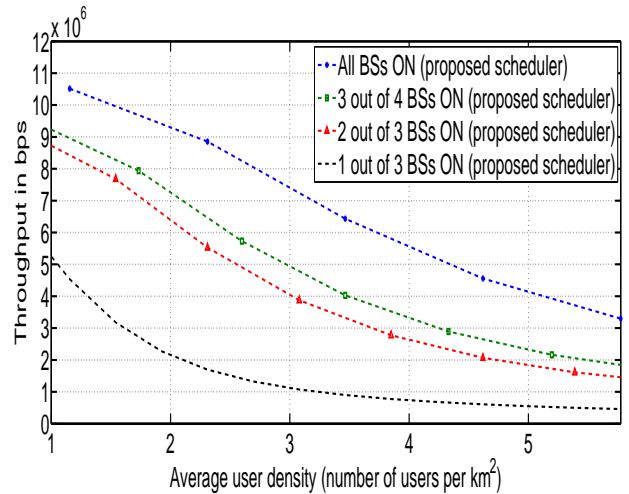


Fig. 7. Geometric mean throughput in the downlink versus average user density for rural macro-cell.

as $P_{UE} = 24$ dBm and $P_{BS} = 46$ dBm, respectively. We consider that each sector of any BS has a total of 33 channels. Thus, $M = 99$. We assume that the system uses adaptive modulation with discrete rates given by the mapping in Table 2. The sub-channel bandwidth, SC_{OFDM} , SY_{OFDM} , and sub-frame duration are taken as 180 KHz, 12, 14, and 1ms, respectively. A downlink and uplink TDD configuration of 3:2 as specified in [4] is considered (i.e., β is equal to 3/5).

We first check that using the proposed schedulers on the nominal system does not provide significant throughput gains. We also verified that the benchmark uplink scheduler do not provide full coverage on any of the considered BSS patterns for both urban and rural macro-cell environments. Then, considering each of the BSS patterns, we determine the value of parameters X and Y for both scenarios. The permissible values of X for the downlink are calculated considering only one UE in the system. A value of $X \in \{1, \dots, M/3\}$ is considered permissible if, given that X , the UE receives full coverage in the downlink at all possible locations on the grid. Then, the optimal value is calculated based on (36) for each BSS pattern. For BSS patterns, $A_{3/4}$, $A_{2/3}$, and $A_{1/3}$, the respective optimal values are $X_{3/4} = 31$, $X_{2/3} = 31$, and $X_{1/3} = 28$. Further, the values are same for both urban and rural settings. Since the value of $X_{e1/e2}$ is high, we believe that our upper bound on interference on the downlink is tight. Similarly, the permissible values of Y in the uplink are calculated. Note that due to the coverage constraint on the uplink, Y is equal to 1 for all the proposed BSS patterns for both scenarios.

For the downlink, in each BSS pattern, we solve the decoupled problem in (27) for a single UE for all possible values of l_n for a sector of the central cell. We calculate the average geometric mean by using the fact that in the downlink the decoupled nature of

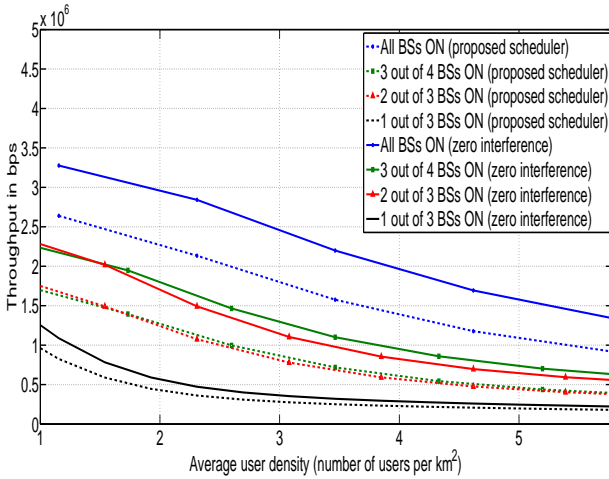


Fig. 8. Geometric mean throughput in the uplink versus average user density for rural macro-cell.

the problem results in

$$E_{\{l_n\}} \left[\left(\prod_{N_s} \lambda^D(l_n) \right)^{\frac{1}{N_s}} \right] = \left(E_{l_n} \left[\lambda^D(l_n)^{\frac{1}{N_s}} \right] \right)^{N_s} \quad (38)$$

$$= \left(\frac{\sum_{l_n=1}^{L_{e1/e2}} \left[\lambda^D(l_n)^{\frac{1}{N_s}} \right]}{L_{e1/e2}} \right)^{N_s}$$

Thus, using (38), we plot the average of GM^D for the BSS patterns for various user densities in Fig. 7 for a rural macro-cell environment, where the average is over all possible UE locations in a sector and 200 realizations are considered for the number of users in the cell, given an average user density. The proposed scheduler allows us to use several BSS patterns as shown in Fig. 7.

Unlike the downlink, on the uplink the optimization problem in (31) cannot be decoupled to a per user problem. The problem in (31) is a mixed integer non-linear program (MINLP). The numerical results are obtained using SCIP [19]. We generate 200 realizations for each BSS pattern, user density, and urban/rural macro-cell environment. Given a realization, we solve the optimization problem in (31) to generate each user's throughput $\lambda^U(l_n)$. The geometric mean throughput $GM^U = \sqrt[N_s]{\prod_{n=1}^{N_s} \lambda^U(l_n)}$ is then calculated on a per realization basis. The average of GM^U is calculated over the 200 realizations to generate each data point in Fig 8, where we plot the variation of the average over 200 realizations of GM^U as a function of user density, for the various BSS patterns. For both uplink and downlink, if the BSS pattern has asymmetric sectors like for $A_{3/4}$, we further average out the results over all three sectors using the set of channels \mathcal{M}_1 , \mathcal{M}_2 , and \mathcal{M}_3 . An important difference between Fig. 7 and Fig. 8 for the rural macro-cell environment is that the performance

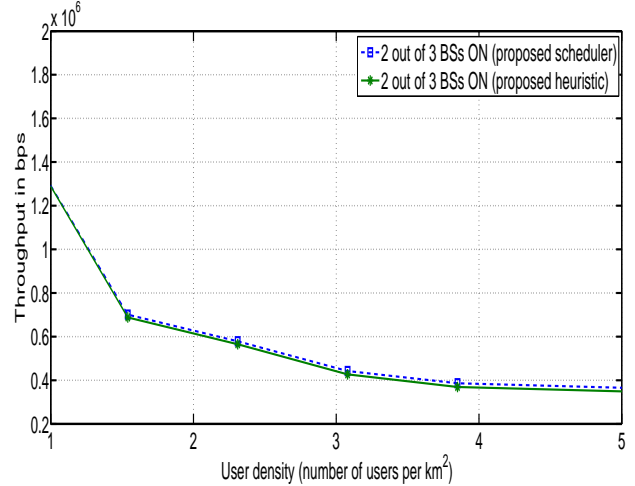


Fig. 9. Comparison of the proposed heuristic and the proposed scheduler with respect to geometric mean throughput versus user density for rural macro-cell.

of the users on the uplink is much more affected when BSs are switched off than on the downlink. This confirms our initial observation that the uplink is the bottleneck when switching off BSs (recall $Y=1$ for all feasible BSS patterns). Similar trends were observed in an urban macro-cell environment for downlink and uplink.

In the proposed uplink scheduler, by assuming interference to be a function of P_{UE}/Y (see (35)), we obtain results which lower bound the performance of an actual cellular system for the following reason. Given a BSS pattern and N_s (typically $N_s \ll M$), either the uplink scheduler of a neighboring cell allocates all the channels to its UEs (because some of these UEs are close to the BS and can afford spreading their transmit powers) and in that case the interference on these channels will be much lower than the interference estimated by our bound or it allocates only a fraction of its channels and produces no interference in the other channels.

In order to get a better understanding of the possible performance, under lower interference, we also present, in Fig. 8, the average geometric mean throughput assuming zero interference in the system for the rural macro-cell environment. The user performance on the uplink of a realistic cellular system will lie in between the results of the proposed scheduler assuming an upper bound on interference and the results obtained by assuming zero interference. It is observed in Fig. 8 that as the number of switched off BSs increases, the gap between the results with and without interference decreases. This can be attributed to the fact that switching off BSs results in larger ISD and the uplink moves from an interference limited to a noise limited system.

The performance of our heuristic for the proposed uplink scheduler is presented in Fig. 9. The heuristic

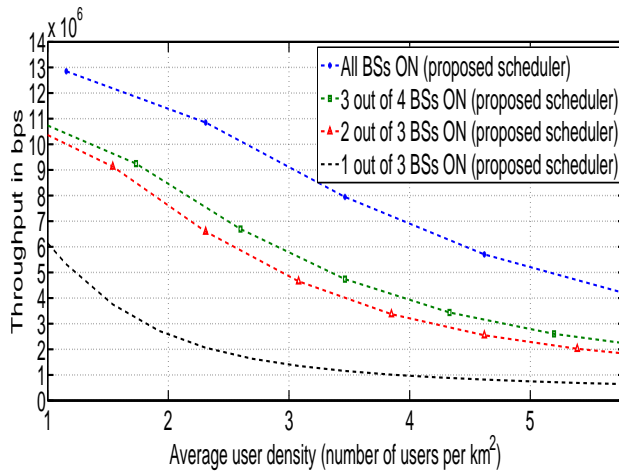


Fig. 10. Combined geometric mean throughput (uplink and downlink combined for $\beta = 3/5$) versus user density for rural macro-cell.

performance is very close to the proposed uplink scheduler for low user density. The gap in performance widens slightly with an increase in user density. However, as the loss in performance is within 1% (for most of the user density scenarios under consideration), our heuristic is a very good approximation of the proposed uplink scheduler with a significantly lower computational cost.

In Fig. 10, we combine the user rates on the uplink and downlink from Fig. 7 and Fig. 8 for β equal to $3/5$ (the downlink time fraction for TDD) for the rural macro-cell environment. Similar results are obtained for an urban macro-cell in Fig. 11 by combining the user rates for downlink and uplink in an urban macro-cell environment. There are two ways a cellular operator could use Fig. 10 and Fig. 11. First, given a user density, she can select the BSS pattern that gives her the performance/energy trade-off that she likes.

In Fig. 12, we present the energy performance trade-off curve for a given average user density of 10 per macro-cell (i.e., 10 users per 2.598 km² for the rural macro-cell and 10 users per 0.2165 km² for the urban macro-cell environment). Using Fig. 12, a cellular operator can trade a decrease of 42% (resp. 53% or 85%) in the per-user (i.e., uplink and downlink combined) geometric mean throughput for saving 25% (resp. 33% or 66%) energy by using BSS pattern $A_{3/4}$ (resp. $A_{2/3}$, or $A_{1/3}$). For the case of urban macro-cell a decrease of 38% (resp. 49% or 59%) in the per-user geometric mean throughput is obtained for saving 25% (resp. 33% or 66%) energy by using BSS pattern $A_{3/4}$ (resp. $A_{2/3}$, or $A_{1/3}$). Clearly, the savings in energy come at a large cost in performance. We have also represented the trade-off points for the benchmark schedulers in Fig. 12. Although, they perform close to the proposed schedulers in the nominal system, they fail to provide full coverage in the other BSS

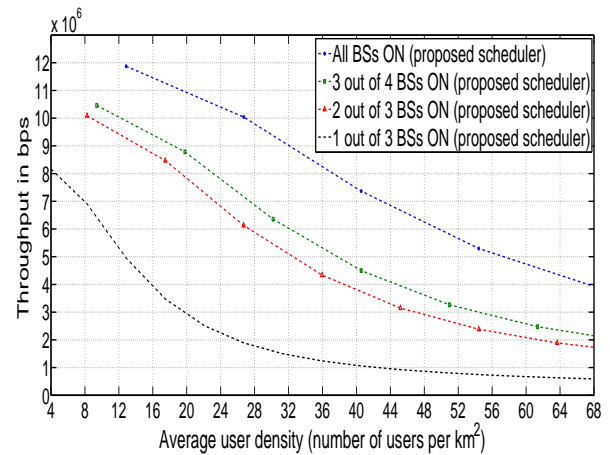


Fig. 11. Combined geometric mean throughput (uplink and downlink combined for $\beta = 3/5$) versus user density for urban macro-cell.

patterns and hence we only have trade-off points for the nominal pattern. Second, given different user densities at different times of the day (e.g., day and night), the operator can select the BSS pattern that allows her to save energy while keeping the average performance approximately constant. For example, in Fig. 10, with a decrease in the average user density from 5 to 3.3 (resp. 2.8 or 1.2) a cellular operator can switch off 1/4 (resp. 1/3 or 2/3) of the total BSs while maintaining the same average per user geometric mean throughput with full coverage and energy saving of the order of 25% (resp. 33% or 66%) for BSS pattern $A_{3/4}$ (resp. $A_{2/3}$, or $A_{1/3}$). Thus, using the proposed schedulers, given a reasonable (predefined) decrease in the user density, cellular operators can switch off BSs and maintain coverage without a loss in the geometric mean throughput.

6 CONCLUSION

We have shown that there is a complex interplay between coverage, power management, scheduling, and interference and that this interplay has to be taken into account carefully to enable base station switching to save energy. We have shown that the limiting factor for switching off BSs, while maintaining coverage, is the uplink. We have proposed flexible schedulers for both uplink and downlink that allow coverage extension by focusing the transmit power on fewer sub-channels. We have also proposed several BSS patterns that offer full coverage when using our schedulers in both urban and rural macro-cell environments. Further, a low complexity high performance heuristic is proposed for the uplink scheduler. All together, base station switching is a simple yet effective technique which can provide significant energy savings without compromising on coverage while maintaining reasonable throughput as long as scheduling is performed

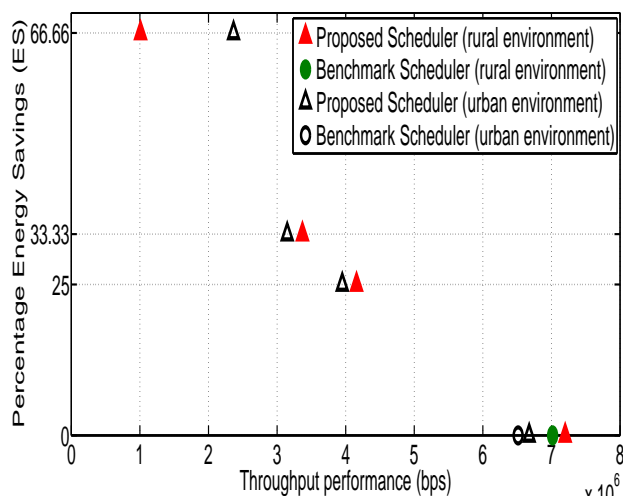


Fig. 12. Energy performance trade-off for the proposed and benchmark scheduler given $\beta = 3/5$ and an average of 10 users per macro-cell.

carefully. Our study is an offline study that does not address the problem of deciding when to change from one BSS pattern to another or back to the nominal scenario. However, BSS switching cannot be done online without pre-computing beforehand which patterns are feasible or not. Thus, the next step would be to decide on-line when to switch from one BSS pattern to another based on user density measurements. This is a possible area of future research. d

REFERENCES

- [1] A. Fehske, G. Fettweis, J. Malmudin, and G. Biczok, "The global footprint of mobile communications: the ecological and economic perspective," *IEEE Communications Magazine*, vol. 49, no. 8, pp. 55–62, 2011.
- [2] G. Auer, V. Gianni, C. Desset, I. Godor, P. Skillermark, M. Olsson, M. A. Imran, D. Sabella, M. J. Gonzalez, O. Blume, and A. Fehske, "How much energy is needed to run a wireless network," *IEEE Wireless Communications*, vol. 18, no. 5, pp. 40–49, 2011.
- [3] 3GPP-TSG-RAN-WG1, "Evolved universal terrestrial radio access (E-UTRA)," *3GPP, Tech. Rep. TR 36.814*, 2010.
- [4] O. Eunsung, B. Krishnamachari, L. Xin, and N. Zhisheng, "Toward dynamic energy-efficient operation of cellular network infrastructure," *IEEE Communications Magazine*, vol. 49, no. 6, pp. 56–61, 2011.
- [5] O. Eunsung, S. Kyuho, and B. Krishnamachari, "Dynamic base station switching-on/off strategies for green cellular networks," *IEEE Transactions on Wireless Communications*, vol. 12, no. 5, pp. 2126–2136, 2013.
- [6] K. Son, H. Kim, Y. Yi, and B. Krishnamachari, "Towards energy-efficient operation of base stations in cellular wireless networks," a book chapter of *Green Communications: Theoretical Fundamentals, Algorithms, and Applications*, CRC Press, Taylor & Francis, 2012.
- [7] Y. Chen, S. Zhang, and S. Xu, "Fundamental trade-offs on green wireless networks," *IEEE Communications Magazine*, vol. 49, no. 6, pp. 30–37, 2011.
- [8] S. Kim, S. Choi, and B. Lee, "A joint algorithm for base station operation and user association in heterogeneous networks," *IEEE Communications Letters*, vol. 17, no. 17, pp. 1552–1555, August 2013.
- [9] W. Guo and T. O'Farrell, "Dynamic cell expansion with self-organizing cooperation," *IEEE Journal on Selected Areas in Communications*, vol. 31, no. 5, pp. 851–860, 2013.

- [10] Z. Niu, Y. Wu, J. Gong, and Z. Yang, "Cell zooming for cost-efficient green cellular networks," *IEEE Communications Magazine*, vol. 48, no. 11, pp. 74–79, 2010.
- [11] H. Chen, Y. Jiang, J. Xu, and H. Hu, "Energy-efficient coordinated scheduling mechanism for cellular communication systems with multiple component carriers," *IEEE Journal on Selected Areas in Communications*, vol. 31, no. 5, pp. 959–968, May 2013.
- [12] M. A. Marsan, L. Chiaraviglio, D. Ciullo, and M. Meo, "Optimal energy savings in cellular access networks," in *Proc. IEEE ICC Workshops*, Dresden, Germany, June 2009, pp. 1–5.
- [13] P. Kolios, V. Friderikos, and K. Papadaki, "Energy-efficient relaying via store-carry and forward within the cell," *IEEE Transaction on Mobile Computing*, vol. 13, no. 1, pp. 202–215, January 2014.
- [14] M. F. Hossain, K. S. Munasinghe, and A. Jamalipour, "Distributed inter-BS cooperation aided energy efficient load balancing for cellular networks," *IEEE Transactions on Wireless Communications*, vol. 12, no. 11, pp. 5929–5939, 2013.
- [15] R. Sappidi, S. Mosharrafdehkhordi, C. Rosenberg, and P. Mitran, "Planning for small cells in a cellular network: why is it worth it," in *Proc. IEEE WCNC 2014*, Istanbul, Turkey, April 2014.
- [16] C. Y. Chang, W. Liao, H. Y. Hsieh, and D. S. Shiu, "On optimal cell activation for coverage preservation in green cellular networks," *IEEE Transactions on Mobile Computing*, vol. PP, no. 99, pp. 1–13, 2014.
- [17] L. Li, M. Pal, and Y. R. Yang, "Proportional fairness in multi-rate wireless LANs," in *Proc. IEEE INFOCOM*, Phoenix, USA, May 2008, pp. 1004–1012.
- [18] D. Lopez-Perez, A. Ladanyi, A. Juttner, and J. Zhang, "Optimization method for the joint allocation of modulation schemes, coding rates, resource blocks and power in self-organizing LTE networks," in *Proc. IEEE INFOCOM*, Shanghai, China, April 2011, pp. 111–115.
- [19] Available: <http://scip.zib.de>.



Abhinav Kumar (S'04–M'14) received the dual degree (with B.Tech. in Electrical Engineering and M.Tech. in Information and Communication Technology) and the Ph.D. degree (in Electrical Engineering) from the Indian Institute of Technology, Delhi, in 2009 and 2013, respectively. From September to November, 2013, he has worked as a research associate at the Indian Institute of Technology, Delhi. From December 2013 to November 2014, he has worked as a Post-doctoral Fellow at the University of Waterloo, Canada. Since November 2014, he has been with Indian Institute of Technology Hyderabad, India, as an Assistant Professor. His research interests are in the different aspects of wireless communications and networking.



Catherine Rosenberg is a Professor in Electrical and Computer Engineering at the University of Waterloo. Since June 2010, she holds the Tier I Canada Research Chair in the Future Internet. From 1999 to 2004, Prof. Rosenberg was a Professor in the School of Electrical and Computer Engineering at Purdue University. Prof. Rosenberg was elected an IEEE Fellow in 2011 and a Fellow of the Canadian Academy of Engineering in 2013. Her research interests are mainly in two areas: the Internet and Energy Systems. Prof. Rosenberg obtained her "Diplome d'Ingénieur" from the Ecole Nationale Supérieure des Télécommunications de Bretagne, her M.S. in Computer Science from the University of California at Los Angeles and her "Doctorat en Sciences" from Université Paris XI.